Articles

Chalcogen-Centered Spirocyclic Mixed-Metal Carbonyl Complexes: Synthesis and Molecular Structures of $(CO)_8(\mu\text{-}PCy_2)Re_2(\mu_4\text{-}E)Fe_2(\mu\text{-}ER)(CO)_6$ and $[(CO)_8(\mu\text{-}PCy_2)Re_2(\mu_4\text{-}E)Fe_2(CO)_6]_2(\mu_4\text{-}E_2)$ (E = S, Se, Te; R = Organic Residue)

Stefanie Klose, Ulrich Flörke, and Hans Egold*

Fakultät für Naturwissenschaften der Universität Paderborn, Department Chemie, Warburgerstrasse 100, D-33098 Paderborn, Germany

Pradeep Mathur

Chemistry Department, Indian Institute of Technology, Bombay, Powai, Bombay 400 076, India

Received March 17, 2003

When $NEt_4[Re_2(\mu\text{-}PCy_2)(CO)_8]$ (**1**) was reacted with $Fe_2(\mu\text{-}E_2)(CO)_6$ (E = S, Se, Te) in THF, the salts $NEt_4[(CO)_8(\mu\text{-}PCy_2)Re_2(\mu_4\text{-}E)Fe_2(\mu\text{-}E)(CO)_6]$ (E = S (**2a**), Se (**2b**), Te (**2c**)) were formed. Their spirocyclic anions were trapped with MeI, giving the spirocyclic complexes $(CO)_8(\mu\text{-}PCy_2)Re_2(\mu_4\text{-}E)Fe_2(\mu\text{-}EMe)(CO)_6$ (E = S (**3a**), Se (**3b**), Te (**3c**)). Their molecular structures were confirmed by single-crystal X-ray analysis. The anions of **2a**−**c** are sensitive to oxidation. On crystallization in the presence of oxygen the corresponding dichalcogenides $[(CO)_8(\mu\text{-}PCy_2)Re_2(\mu_4\text{-}E)Fe_2(CO)_6]_2(\mu_4\text{-}E_2)$ (E = S (**4a**), Se (**4b**), Te (**4c**)) were obtained in good yield. Their molecular structures were confirmed by single-crystal X-ray analysis. **2a** was also trapped with CF_3COOH, giving $(CO)_8(\mu\text{-}PCy_2)Re_2(\mu\text{-}S_4)Fe_2(\mu\text{-}SH)(CO)_6$ (**5**). The latter can be expanded by SH oxidative addition of its μ-SH function to $Os_3(CO)_{11}(NCMe)$, giving the mixed-metal carbonyl complex $(CO)_8(\mu\text{-}PCy_2)Re_2(\mu_4\text{-}S)Fe_2(CO)_6(\mu_3\text{-}S)Os_3(\mu\text{-}H)(CO)_{11}$ (**6**). The framework of **6** could be derived from X-ray diffraction data. However, these data were insufficient for complete solution of the molecular structure, but spectroscopic data and elemental analysis of **6** are in accordance with the proposed molecular structure.

Introduction

Spirocyclic iron carbonyl complexes such as, for example, $(\mu_4\text{-}S)[Fe_2(\mu\text{-}SR)(CO)_6]$, are well-known in organometallic chemistry. The spiro atom in such complexes can be varied over a wide range from being a formally four-electron-donor ligand (Si, Ge, Sn, Pb)[1−3] to a five-electron-donor ligand (P, As, Sb)[4,5] and a six-electron-donor ligand (S, Se, Te),[6−8] respectively. This broad scope of possibilities is based on the high electronic and steric flexibility of the diiron subunits.[3] Many of these complexes exhibit noticeable distortions from the expected regular geometries due to the need to minimize nonbonded interactions between CO groups of neighboring diiron subunits. In most cases this is manifested in a deviation of the dihedral angles Fe_2Y/YFe_2 (Y = spiro atom and main-group element) from

(1) Anema, S. G.; Barris, G. C.; Mackay, K. M.; Nicholson, B. K. *J. Organomet. Chem.* **1988**, *350*, 207.
(2) Whitmire, K. H.; Lagrone, C. B.; Churchill, M. R.; Fettinger, J. C.; Robinson, B. H. *Inorg. Chem.* **1987**, *26*, 3491.
(3) Anema, S. G.; Mackay, K. M.; Nicholson, B. K. *Inorg. Chem.* **1989**, *28*, 3158.
(4) Huttner, G.; Mohr, G.; Pritzlaff, B.; Von Seyerl, J.; Zsolnai, L. *Chem. Ber.* **1982**, *115*, 2044.
(5) (a) Rheingold, A. L.; Geib, S. J.; Shieh, M.; Whitmire, K. H. *Inorg. Chem.* **1987**, *26*, 463. (b) Arif, A. M.; Cowley, A. H.; Pakulski, M. *J. Chem. Soc., Chem. Commun.* **1987**, 622. (c) Ferrer, M.; Rossell, O.; Seco, M.; Braunstein, P. *J. Organomet. Chem.* **1989**, *364*, C5.
(6) Recent examples: (a) Song, L.-C.; Lu, G.-L.; Hu, Q.-M.; Yang, J.; Sun, J. *J. Organomet. Chem.* **2001**, *623*, 56. (b) Song, L.-C.; Hu, Q.-M.; Fan, H.-T.; Sun, B.-W.; Tang, M.-Y.; Chen, Y.; Sun, Y.; Sun, C.-X.; Wu, Q.-J. *Organometallics* **2000**, *19*, 3909. (c) Zheng, H.-B.; Miao, S.-B.; Wang, Z.-X.; Zhou, Z.-Y.; Zhou, X.-G. *Polyhedron* **2000**, *19*, 713. (d) Wang, Z.-X.; Jia, C.-S.; Zhou, Z.-Y.; Zhou, X.-G. *J. Organomet. Chem.* **2000**, *601*, 108. (e) Song, L.-C.; Lu, G.-L.; Hu, Q.-M.; Fan, H.-T.; Chen, Y.; Sun, J. *Organometallics* **1999**, *18*, 3258.
(7) (a) Song, L.-C.; Yang, J.; Hu, Q.-M.; Wu, Q.-J. *Organometallics* **2001**, *20*, 3293. (b) Wang, Z.-X.; Zhao, H.; Zhou, Z.-Y.; Zhou, X.-G. *J. Organomet. Chem.* **2000**, *599*, 256. (c) Song, L.-C.; Qin, X.-D.; Hu, Q.-M.; Huang, X.-Y. *Organometallics* **1998**, *17*, 5437. (d) Song, L.-C.; Yan, C.-G.; Hu, Q.-M.; Wang, R.-J.; Mak, T. C. W.; Huang, X.-Y. *Organometallics* **1996**, *15*, 1535. (e) Mathur, P.; Trivedi, R.; Satyanarayana, C. V. V. *Organometallics* **1996**, *15*, 1062. (f) Song, L.-C.; Yan, C.-G.; Hu, Q.-M.; Huang, X.-Y. *J. Organomet. Chem.* **1995**, *505*, 119.
(8) (a) Nekhaev, A. I.; Kolobkov, B. I.; Aleksandrov, G. G.; Parpiev, N. A.; Tashev, M. T.; Dustov, K. B. *Koord. Khim.* **1988**, *14*, 273. (b) Nekhaev, A. I.; Kolobkov, B. I.; Semenov, I. P.; Aleksandrov, G. G.; Tashev, M. T.; Dustov, K. B. *Izv. Akad. Nauk SSSR, Ser. Khim.* **1987**, 458.

10.1021/om030200u CCC: $25.00
Publication on Web 07/24/2003

the expected 90° angle. The obtained molecules are often chiral, and in some cases enantiomerically pure single crystals due to natural resolution of the isomers were found.[9] Mixed-metal spirocyclic carbonyl complexes as compared to the above-described iron complexes are rare. So far only the following examples are known: $[(CO)_6(\mu\text{-}CO)Co_2(\mu_4\text{-}Ge)]_2Fe_2(\mu\text{-}CO)(CO)_7$,[10] $(CO)_8FeW(\mu_4\text{-}P)Fe_2(\mu\text{-}Br)(CO)_6$,[11] $(CO)_8(\mu\text{-}H)Re_2(\mu_4\text{-}S)Os_3(\mu\text{-}H)(CO)_{10}$,[12] $[(CO)_8(\mu\text{-}H)Re_2(\mu_4\text{-}S)]_2M_2(CO)_6$ (M = Fe, Co),[12] $(CO)_8(\mu\text{-}H)Re_2(\mu_4\text{-}S)Ru_2(\mu\text{-}C_5H_4N)(CO)_6$,[13] $(CO)_7(\mu,\eta^2\text{-}pyS)Re_2(\mu_4\text{-}S)Ru_2(\mu\text{-}C_5H_4N)(CO)_6$ (pyS = thiopyridyl),[13,14] $(CO)_8ReRu(\mu_4\text{-}S)Ru_2(\mu\text{-}C_5H_4N)(CO)_6$,[14] and $Fe_2M_3(\mu_4\text{-}E)(\mu_3\text{-}E')(CO)_{17}$ (M = Ru, Os; E = S, Se, Te; E′ = Se, Te).[15] The selective preparation of such mixed-metal complexes is difficult and so far best performed by oxidative addition of μ-YH or μ-YH_2 complexes to certain reactive metal carbonyl complexes. A typical example is the SH oxidation of $Re_2(\mu\text{-}H)(\mu\text{-}SH)(CO)_8$ to $Os_3(CO)_{11}(NCMe)$, giving $(CO)_8(\mu\text{-}H)Re_2(\mu_4\text{-}S)Os_3(\mu\text{-}H)(CO)_{10}$ in high yield.[12]

This paper deals with the selective, high-yield synthesis of chalcogen-centered mixed rhenium iron spirocyclic complexes and describes an attempt to expand one of these complexes by SH oxidative addition to $Os_3(CO)_{11}(NCMe)$.

Results and Discussion

1. Synthesis and Characterization of $(CO)_8(\mu\text{-}PCy_2)Re_2(\mu\text{-}E_4)Fe_2(\mu\text{-}EMe)(CO)_6$ (E = S (3a), Se (3b), Te (3c)). The anion of the salt $NEt_4[Re_2(\mu\text{-}PCy_2)(CO)]_8$ (**1**) is a well-known nucleophile.[16] It reacts easily with many electrophiles such as $ClCuPPh_3$,[17] $HgCl_2$,[18] and $[Rh(COD)][ClO_4]$[19] to give trinuclear heterometallic complexes such as, for example, $Re_2(CuPPh_3)(\mu\text{-}PCy_2)(CO)_8$.[17] Song et al. have shown that similar anionic iron carbonyl complexes such as $[Fe_2(\mu\text{-}ER)(\mu\text{-}CO)(CO)_6]^-$ (E = S, Se, Te) are highly reactive toward the electrophilic diiron complex $Fe_2(\mu\text{-}E'_2)(CO)_6$ (E′ = S, Se).[6,7a] The products resulting from these reactions are butterfly complexes that are linked into a chain by a spiro atom, such as, for example, in $[(CO)_6(\mu\text{-}SBu^t)Fe_2(\mu_4\text{-}S)Fe_2(\mu\text{-}S)(CO)_6]^-$.[6a] In an attempt to prepare mixed-metal spirocyclic complexes, we adapted this synthetic procedure by reacting **1** with $Fe_2(\mu\text{-}E_2)(CO)_6$ (E = S, Se, Te) in THF at −78 °C (Scheme 1, step **i**). The reactions lead to the formation of the salts $NEt_4[(CO)_8(\mu\text{-}PCy_2)Re_2(\mu_4\text{-}E)Fe_2(\mu\text{-}E)(CO)_6]$ (E = S (**2a**), Se (**2b**), Te (**2c**)). For E = S the reaction was followed by ν_{CO} IR spectra and ^{31}P NMR spectra, proving that within minutes an almost quantitative reaction takes place. It must be pointed out that the choice of nucleophile is crucial for the success of this type of reaction. The analogous experiment with the less nucleophilic $NEt_4[Mn_2(\mu\text{-}PCy_2)(CO)_8]$ instead of **1** gives no reaction. **2a** was characterized by its in situ ν_{CO} IR and ^{31}P NMR spectra. The latter exhibits a characteristic resonance at δ −76.0, proving the formation of an Re_2 edge bridged by a μ-PR_2 ligand and a μ-S ligand with no bonding Re−Re interaction.[20] **2b**,**c** are extremely sensitive toward oxygen and were therefore not spectroscopically characterized. However, the structures of all spirocyclic anions have been derived from the full characterization of their derivatives **3a**−**c** and **4a**−**c**, respectively. The orange compounds $(CO)_8(\mu\text{-}PCy_2)Re_2(\mu_4\text{-}E)Fe_2(\mu\text{-}EMe)(CO)_6$ (E = S (**3a**), Se (**3b**), Te (**3c**)) are formed in high yield from the reaction of in situ prepared **2a**−**c** with MeI (Scheme 1, step **ii**).

Scheme 1

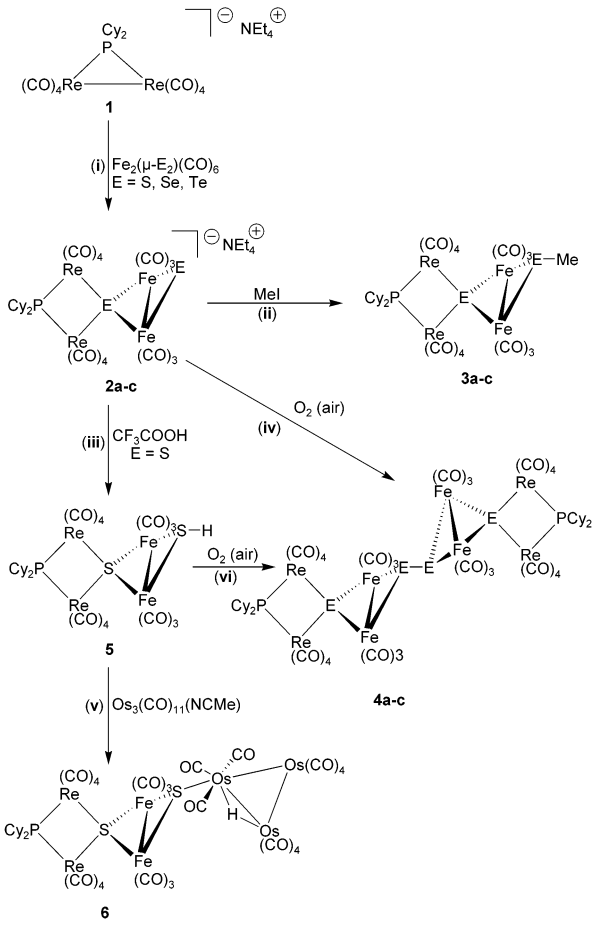

Molecular Structures of 3a−c. These three compounds are isostructural, differing only in the substitution of the μ_4-E bridging atom S, Se, and Te, respectively. The following discussion focuses on the tellurium compound **3c** (Figure 1; **3a**,**b** are not depicted), but it should be mentioned that the triclinic crystal packing of **3c** differs from that of **3a**,**b**, which are isotypic with a monoclinic unit cell.

(9) (a) Song, L.-C.; Yan, C.-G.; Hu, Q.-M.; Wang, R.-J.; Mak, T. C. W.; Huang, X.-Y. *Organometallics* **1996**, *15*, 1535. (b) Song, L. C.; Kadiata, M.; Wang, J.-T.; Wang, R.-J.; Wang, H.-G. *J. Organomet. Chem.* **1988**, *340*, 239.

(10) Anema, S. G.; Audett, J. A.; Mackay, K. M. *J. Chem. Soc., Dalton Trans.* **1988**, 2629.

(11) Lang, H.; Huttner, G.; Zsolnai, L.; Mohr, G.; Sigwarth, B.; Weber, U.; Orama, O.; Jibril, I. *J. Organomet. Chem.* **1986**, *304*, 157.

(12) Egold, H.; Schwarze, D.; Schraa, M.; Flörke, U. *J. Chem. Soc., Dalton Trans.* **2000**, 4385.

(13) Cockerton, B. R.; Deeming, A. J. *Polyhedron* **1994**, *13*, 1945.

(14) Cockerton, B. R.; Deeming, A. J.; Mazurul, K.; Hardcastle, K. I. *J. Chem. Soc., Dalton Trans.* **1991**, 431.

(15) (a) Mathur, P.; Payra, P.; Ghose, S.; Hossain, M. M.; Satyanarayana, C. V. V.; Chicote, F. O.; Chadha, R. K. *J. Organomet. Chem.* **2000**, *606*, 176. (b) Mathur, P.; Hossain, M. M.; Rashid, R. S. *J. Organomet. Chem.* **1993**, *460*, 83. (c) Mathur, P.; Mavunkal, I. J.; Rugmini, V. *Inorg. Chem.* **1989**, *28*, 3616.

(16) Haupt, H.-J.; Disse, G.; Flörke, U. *Z. Anorg. Allg. Chem.* **1994**, *620*, 1664.

(17) Flörke, U.; Haupt, H. J. *Z. Kristallogr.* **1992**, *201*, 323.

(18) Haupt, H. J.; Merla, A.; Flörke, U. *Z. Anorg. Allg. Chem.* **1994**, *620*, 999.

(19) Haupt, H.-J.; Wittbecker, R.; Florke, U. *Z. Anorg. Allg. Chem.* **2001**, *627*, 472.

(20) Egold, H.; Klose, S.; Flörke, U. *Z. Anorg. Allg. Chem.* **2001**, *627*, 164.

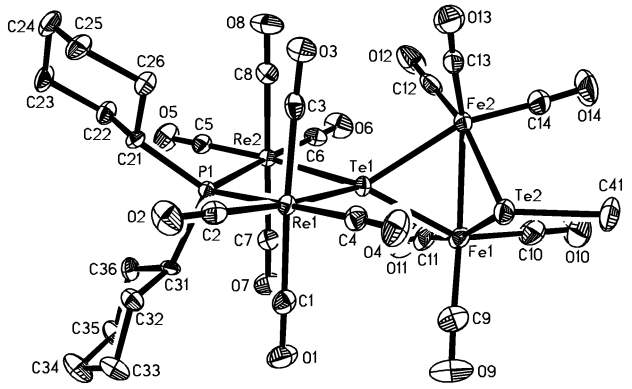

Figure 1. Molecular structure of **3c** with 50% probability ellipsoids. Hydrogen atoms are omitted.

3c shows a central bridgehead μ_4-Te(1) atom which connects a Re_2P moiety with an $Fe_2Te(2)$ one. Each Re atom is attached to four CO groups, the bridging μ-PCy_2 ligand, and the μ_4-Te and thus attains a slightly distorted tetrahedral coordination. The CO groups at the Re atoms have an eclipsed arrangement with C−Re−Re−C torsion angles that range from 0.0 to 6.0° (absolute values). The PRe_2Te1 plane is not planar but folded along the Re···Re vector with a dihedral angle PRe_2/Re_2Te of 12.75(6)° (12.4(1)° for **3a** and 9.8(1)° for **3b**). Both Fe atoms show distorted-octahedral coordination patterns. Each Fe atom has three CO ligands with an eclipsed arrangement, resulting in C−Fe−Fe−C torsion angles from 2.3 to 3.1°. Additionally, each Fe atom is connected to the μ_4-Te and to the μ_2-Te(2) atom with its terminal methyl group. The two $Fe_2Te(1)$ and $Fe_2Te(2)$ planes form a dihedral angle of 79.72(2)° (81.7(1)° and 82.08(6)° for **3a**,**b**, respectively). Finally, the spirocyclic center E = Te shows an almost ideal geometry with an angle of 86.34(1)° between the Re_2Te and $TeFe_2$ planes (86.11(7)° for E = S, **3a**; 86.75(4)° for E = Se, **3b**). The Te−Re and Te−Fe bond lengths differ slightly, with values of 2.7811(3) Å (Re1) and 2.7864(3) Å (Re2) or 2.5432(7) Å (Fe1) and 2.5552(6) Å (Fe2). The Te−Re bonds are thus somewhat shorter than those in (μ_4-Te)[Re_2(μ-SePh)$(CO)_8$]$_2$ at 2.8120(7) Å.[26] In **3b** and **3a** the corresponding distances E−Re1, −Re2, −Fe1, and −Fe2 are as follows: for E = Se, 2.6270(11), 2.6585(10), 2.4139(15), and 2.3924(15) Å; for E = S,: 2.535(3), 2.575(2), 2.320(3), and 2.290(3) Å. The Fe−Fe bond length increases with E from 2.537(2) Å (S) to 2.576(2) Å (Se) and 2.6476(9) Å (Te), and the Re−E−Re and Fe−E−Fe angles decrease in the same order (see Table 3).

Spectroscopic Properties of 3a−c. The IR spectra of **3a−c** display six ν_{CO} absorption bands. Their pattern looks like a superposition of the ν_{CO} IR spectra of Re_2(μ-PCy_2)(μ-SPh)$(CO)_8$[20] and Fe_2(μ-SPh)$_2(CO)_6$.[21] The ^{1}H NMR spectra exhibit the resonances of the methyl groups at δ 2.18 (**3a**), 2.16 (**3b**), and 2.20 (**3c**), in good agreement with the chemical shift of this group in similar molecules.[6b,7a,25] The corresponding ^{13}C NMR resonances are located at δ 19.5 (**3a**), 8.7 (**3b**), and −13.8 (**3c**). The high-field shift of this signal is in accordance with an increasing electron density induced by the heavier chalcogen atoms. The molecular structures of **3a−c** show the methyl group pointing away from the dirhenium subunit (exo orientation). On the basis of the NMR data the existence of a hypothetical isomer with a methyl group pointing toward the dirhenium fragment (endo isomer) cannot be excluded, since both isomers may be rapidly interconverting, giving the same number of resonances as expected for only one isomer. However, with respect to the molecular structures of **3a−c** the existence of the endo isomer is very unlikely, due to intramolecular steric hindrance. It must be pointed out that the ^{13}C NMR spectra of **3a−c** exhibit the expected six resonances of the CO ligands coordinated to rhenium (range of δ 184−193), but only two resonances for the CO ligands coordinated to iron (range of δ 208−211), although according to the X-ray structures three resonances would have been expected. We ascribe this observation to a fast fluxional process of the CO ligands. For the cyclohexyl rings six resonances are observed instead of the usually expected four, strongly pointing toward a hindered rotation about the P−C bond, making C^2, C^6 and C^3, C^5, respectively, distinguishable. The ^{31}P NMR resonances of the phosphido bridge at δ −78.1 (**3a**), −89.1 (**3b**), and −115.3 (**3c**) prove that there is no bonding interaction between the two rhenium atoms. Their high-field shift is characteristic for such complexes, as shown by comparison with the corresponding resonances of the complexes Re_2(μ-PCy_2)(μ-EPh)$(CO)_8$ (δ(μ-P) ($CDCl_3$): −101.2 (E = S), −116.2 (E = Se), −147.9 (E = Te)).[20]

2. Oxidation of in Situ Prepared NEt_4[$(CO)_8$(μ-PCy_2)Re_2(μ_4-E)Fe_2(μ-E)$(CO)_6$] (E = S (2a), Se (2b), Te (2c)). Solutions of NEt_4[$(CO)_8$(μ-PCy_2)Re_2(μ_4-E)Fe_2-(μ-E)$(CO)_6$] (E = S (**2a**), Se (**2b**), Te (**2c**)) are very sensitive with respect to oxidation. Upon concentration under reduced pressure and subsequent crystallization by diffusion of pentane into a THF solution in the presence of aerial oxygen, the dichalcogenides [$(CO)_8$-(μ-PCy_2)Re_2(μ_4-E)$Fe_2(CO)_6]_2$(μ_4-E_2) (E = S (**4a**), Se (**4b**), Te (**4c**)) were obtained in high yield (Scheme 1, step **iv**). **4a** is completely insoluble in all common organic solvents. Therefore, it could only be characterized by ν_{CO} IR spectra (KBr pellet) and elemental analysis. However, its molecular structure has been confirmed by single-crystal X-ray analysis. **4b**,**c** are soluble in THF, $CHCl_3$, and CH_2Cl_2. As expected, the patterns of the ν_{CO} IR spectra of **4a−c** are completely analogous to those of **3a−c**. The ^{31}P NMR spectra of **4b**,**c** exhibit resonances at δ −83.8 (**4b**) and −111.5 (**4c**), respectively, in compliance with the observed resonances of **3b**,**c** (compare discussion above). The molecular structures of both complexes were verified by single-crystal X-ray analysis.

Molecular Structures of 4a−c. This is another series of isomolecular compounds with different E = S (**4a**), Se (**4b**), and Te (**4c**) atoms. Crystal packing is different, as well, as the molecules of **4b**,**c** each occupy a special position of crystallographic inversion center in the triclinic space group $P\bar{1}$, whereas **4a** lies on a

(21) Adeleke, J. A.; Chen, Y. W.; Liu, L. K. *Organometallics* **1992**, *11*, 2543.
(22) Kuwata, S.; Hidai, M. *Coord. Chem. Rev.* **2001**, *213*, 211.
(23) (a) Hieber, W.; Gruber, J. *Z. Anorg. Allg. Chem.* **1958**, *296*, 91. (b) Mathur, P.; Sekar, P.; Satyanarayana, C. V. V.; Mahon, M. F. *Organometallics* **1995**, *14*, 2115. (c) Mathur, P.; Chakrabaty, D.; Hossain, M. M.; Rashid, R. S. *J. Organomet. Chem.* **1991**, *420*, 79.
(24) Nicholls, J. N.; Vargas, M. D. *Inorg. Synth.* **1989**, *26*, 289.
(25) Mathur, P.; Reddy, V. D.; Das, K.; Sinha, U. C. *J. Organomet. Chem.* **1991**, *409*, 255.
(26) Egold, H.; Flörke, U. *Z. Anorg. Allg. Chem.* **2001**, *627*, 2295.

Table 1. Crystallographic Data

	3a	3b	3c
formula	$C_{27}H_{25}Fe_2O_{14}PRe_2S_2$	$C_{27}H_{25}Fe_2O_{14}PRe_2Se_2$	$C_{27}H_{25}Fe_2O_{14}PRe_2Te_2$
fw	1152.7	1246.5	1343.7
cryst syst	monoclinic	monoclinic	triclinic
space group	$P2_1/c$	$P2_1/c$	$P\bar{1}$
temp/K	203(2)	293(2)	173(2)
a/Å	9.766(5)	9.857(3)	9.2896(4)
b/Å	17.954(2)	18.234(3)	13.0401(6)
c/Å	20.300(2)	20.473(5)	15.93c(8)
α/deg			68.577(1)
β/deg	93.73(3)	93.25(2)	87.538(1)
γ/deg			89.335(1)
V/Å^3	3551.8(19)	3673.7(16)	1801.63(14)
Z	4	4	2
D_{calcd}/g cm^{-3}	2.156	2.254	2.477
μ(Mo Kα)/mm^{-1}	7.82	9.43	9.18
F(000)	2192	2336	1240
scan range *θ*/deg	2.0−27.5	2.2− 27.5	1.7−28.3
no. of measd/unique rflns	10 188/8166	10 487/8427	10 231/7365
R1[a]/wR2[b]	0.052/0.070	0.048/0.093	0.024/0.057
GOF	0.988	1.001	1.015
min/max Δ*F*/e Å^{-3}	−0.94/0.92	−0.98/0.91	−0.91/0.98

[a] $R1(F > 4\sigma(F)) = \sum||F_o| - |F_c||/\sum|F_o|$. [b] $wR2(F^2, \text{all data}) = [\sum w(F_o^2 - F_c^2)^2/\sum w(F_o^2)^2]^{1/2}$.

Table 2. Crystallographic Data

	4a	4b	4c
formula	$C_{52}H_{44}Fe_4O_{28}P2Re_4S_4 \cdot 0.5\ CH_2Cl_2$	$C_{52}H_{44}Fe_4O_{28}P2Re_4Se_4$	$C_{52}H_{44}Fe_4O_{28}P2Re_4Te_4$
fw	2317.7	2462.8	2657.4
cryst syst	monoclinic	triclinic	triclinic
space group	$P2_1/c$	$P\bar{1}$	$P\bar{1}$
temp/K	203(2)	173(2)	173(2)
a/Å	14.793(3)	9.3334(7)	9.351(2)
b/Å	15.605(5)	11.9734(9)	12.026(3)
c/Å	32.027(9)	17.0212(13)	17.270(4)
α/deg		69.958(2)	108.910(4)
β/deg	102.01(1)	79.061(1)	90.285(4)
γ/deg		77.534(1)	102.955(4)
V/Å^3	7231(3)	1730.9(2)	1784.0(7)
Z	4	1	1
D_{calcd}/g cm^{-3}	2.129	2.363	2.473
μ(Mo Kα)/mm^{-1}	7.72	10.00	9.27
F(000)	4396	1150	1222
scan range *θ*/deg	2.1−27.5	1.8−28.3	2.5−28.2
no. of measd/unique rflns	17 654/15 065	11 004/7669	11 021/7833
R1[a]/wR2[b]	0.059/0.148	0.034 / 0.056	0.059/0.127
GOF	0.927	0.778	0.888
min/max Δ*F*/e Å^{-3}	−0.54/0.83	−0.93/1.54[c]	−0.87/1.38[c]

[a] $R1(F > 4\sigma(F)) = \sum||F_o| - |F_c||/\sum|F_o|$. [b] $wR2(F^2, \text{all data}) = [\sum w(F_o^2 - F_c^2)^2/\sum w(F_o^2)^2]^{1/2}$. [c] Near Re position.

general position in the monoclinic space group $P2_1/c$. The following description of the molecular structure focuses on the Se compound **4b** (Figure 2; best refinement results, **4c** is not depicted). The molecule consists of two symmetry-related **3b** units where both μ-Se atoms are linked to each other and the terminal methyl groups of **3b** are dropped. The crystallographic inversion center lies in the middle of the resulting Se−Se bond of 2.4383(12) Å. The **3b** subunit resembles the geometry as discussed above, as may be seen from the following dihedral angles: PRe_2/Re_2Se1, 16.03(9)°; $Re_2Se1/Se1Fe_2$, 85.13(3)°; $Se1Fe_2/Fe_2Se2$, 80.88(3)°. The corresponding values for the S (**4a**) and Te (**4c**) compounds are respectively as follows: 26.9(2) (av), 79.3(1) (av), 83.7(1)° (av); 16.7(1), 83.85(5), 82.10(7)°. Due to the point group symmetry the Fe1−E2−E2a−Fe1a torsion angles are 180° for E = Se, Te but is 152.6° for the S compound (Figure 3). This indicates a strong intramolecular distortion and is due to the short S2−S3 distance of 2.127(5) Å (Se−Se = 2.4383(12), Te−Te = 2.8075(18) Å) and resulting intramolecular repulsion from carbonyl groups attached to Re1 and Fe3,4 or Re3 and Fe1,2. With the observed torsion angle of 152.6° in **4a** the shortest nonbonding O···O distances of these ligands are about 3.0 Å, but with an "ideal" 180° angle valid for **4b**,**c**, these contacts would be as short as 1.6 Å.

3. Formation of $(CO)_8(\mu\text{-}PCy_2)Re_2(\mu\text{-}S_4)Fe_2(\mu\text{-}SH)(CO)_6$ (5) and Its Expansion with $Os_3(CO)_{10+n}(NCMe)_{2-n}$ (n = 0, 1). The hydrogen sulfido bridged complex $(CO)_8(\mu\text{-}PCy_2)Re_2(\mu_4\text{-}S)Fe_2(\mu\text{-}SH)(CO)_6$ (**5**) is formed when **2a** is treated with CF_3COOH. Attempts to prepare analogous selenium and tellurium compounds by treating **2b**,**c**, respectively, with CF_3COOH were unsuccessful, giving the dichalcogenides **4b**,**c**. The spectroscopic features of **5** are almost identical with those of **3a**. However, the ^{13}C NMR spectrum shows two significant differences. First there are only five resonances for the CO ligands coordinated to rhenium. Comparison of their relative intensities with those of **3a** suggests that this observation is explained by a random degeneracy of two resonances. Second, for the CO ligands attached to iron only one resonance is found,

Table 3. Selected Bond Lengths (Å) and Angles (deg)

	Compound **3a**		
Re1−P1	2.519(2)	Re2−P1	2.523(2)
Re1−S1	2.535(3)	Re2−S1	2.575(2)
Fe1−S1	2.320(3)	Fe1−S2	2.250(3)
Fe2−S1	2.290(3)	Fe2−S2	2.254(3)
Fe1−Fe2	2.537(2)		
Re1−P1−Re2	101.51(9)	Re1−S1−Re2	99.66(8)
P1−Re1−S1	79.26(8)	P1−Re2−S1	78.45(8)
Fe1−S1−Fe2	66.78(8)	Fe1−S2−Fe2	68.56(9)
	Compound **3b**		
Re1−P1	2.512(2)	Re2−P1	2.534(2)
Re1−Se1	2.6270(11)	Re2−Se1	2.6585(10)
Fe1−Se1	2.4139(15)	Fe1−Se2	2.3599(19)
Fe2−Se1	2.3924(15)	Fe2−Se2	2.3620(17)
Fe1−Fe2	2.576(2)		
Re1−P1−Re2	103.94(8)	Re1−Se1−Re2	98.20(3)
P1−Re1−Se1	78.99(6)	P1−Re2−Se1	78.18(5)
Fe1−Se1−Fe2	64.82(5)	Fe1−Se2−Fe2	66.13(6)
	Compound **3c**		
Re1−P1	2.551(1)	Re2−P1	2.543(1)
Re1−Te1	2.7811(3)	Re2−Te1	2.7864(3)
Fe1−Te1	2.5432(7)	Fe1−Te2	2.5448(7)
Fe2−Te1	2.5552(7)	Fe2−Te2	2.5422(7)
Fe1−Fe2	2.6476(9)		
Re1−P1−Re2	107.78(4)	Re1−Te1−Re2	95.339(9)
P1−Re1−Te1	77.85(2)	P1−Re2−Te1	77.89(2)
Fe1−Te1−Fe2	62.57(2)	Fe1−Te2−Fe2	62.73(2)
	Compound **4a**		
Re1−P1	2.526(4)	Re2−P1	2.532(4)
Re1−S1	2.551(4)	Re2−S1	2.552(4)
Re3−P2	2.528(4)	Re4−P2	2.524(4)
Re3−S4	2.580(4)	Re4−S4	2.547(4)
Fe1−S1	2.293(4)	Fe1−S2	2.276(4)
Fe2−S1	2.315(4)	Fe2−S2	2.237(5)
Fe3−S3	2.273(5)	Fe3−S4	2.284(4)
Fe4−S3	2.250(4)	Fe4−S4	2.320(5)
Fe1−Fe2	2.517(3)	Fe3−Fe4	2.497(3)
S2−S3	2.127(5)		
Re1−S1−Re2	100.59(12)	Fe1−S1−Fe2	66.22(12)
Fe1−S2−Fe2	67.81(14)	Fe3−S3−Fe4	67.03(14)
Fe3−S4−Fe4	65.69(13)	Re3−S4−Re4	100.08(13)
	Compound **4b**		
Re1−P1	2.5350(16)	Re2−P1	2.5401(16)
Re1−Se1	2.6435(6)	Re2−Se1	2.6529(6)
Fe1−Se1	2.4036(11)	Fe2−Se1	2.4034(10)
Fe1−Se2	2.3627(11)	Fe2−Se2	2.3550(11)
Fe1−Fe2	2.5947(13)	Se2−Se2a	2.4383(12)
Re1−P1−Re2	104.98(6)	Re1−Se1−Re2	98.95(2)
P1−Re1−Se1	77.26(4)	P1−Re2−Se1	77.00(4)
Fe1−Se1−Fe2	65.34(3)	Fe1−Se2−Fe2	66.73(3)
	Compound **4c**		
Re1−P1	2.543(4)	Re2−P1	2.566(4)
Re1−Te1	2.7572(11)	Re2−Te1	2.7736(10)
Fe1−Te1	2.537(2)	Fe2−Te1	2.5438(19)
Fe1−Te2	2.531(2)	Fe2−Te2	2.523(2)
Fe1−Fe2	2.656(3)	Te2−Te2a	2.8075(18)
Re1−P1−Re2	107.98(12)	Re1−Te1−Re2	96.72(3)
P1−Re1−Te1	77.02(8)	P1−Re2−Te1	76.35(8)
Fe1−Te1−Fe2	63.04(6)	Fe1−Te2−Fe2	63.40(6)

indicating a rapid interchange of all of these ligands on each iron atom. The existence of a μ-SH ligand is proved by the ^{1}H NMR resonance of the respective hydrogen atom at δ −0.58. Its chemical shift is characteristic for hydrogen sulfido bridged complexes.[22] All attempts to crystallize **5** failed. Upon crystallization in the presence of oxygen **5** is oxidized at its μ-SH function, giving deep red crystals of the disulfide $[(CO)_8(\mu\text{-}PCy_2)Re_2(\mu_4\text{-}S)Fe_2(CO)_6]_2(\mu_4\text{-}S_2)$ (**4a**; Scheme 1, step **vi**).

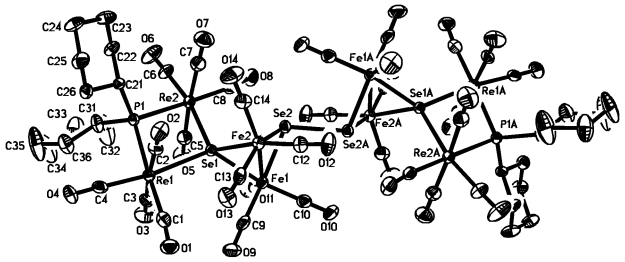

Figure 2. Molecular structure of **4b** with 50% probability ellipsoids. Hydrogen atoms are omitted.

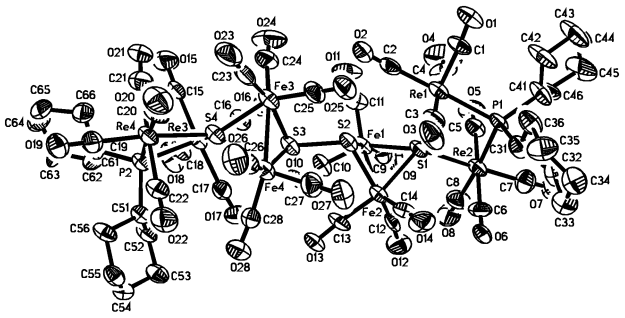

Figure 3. Molecular structure of **4a** with 50% probability ellipsoids. Hydrogen atoms are omitted.

When **5** is treated with equimolar amounts of $Os_3(CO)_{11}(NCMe)$ or $Os_3(CO)_{10}(NCMe)_2$, respectively, the mixed-metal spirocyclic complex $(CO)_8(\mu\text{-}PCy_2)Re_2(\mu_4\text{-}S)Fe_2(CO)_6(\mu_3\text{−}S)Os_3(\mu\text{-}H)(CO)_{11}$ (**6**) is obtained by SH oxidative addition of the hydrogen sulfido bridge to the triosmium complex in a yield of 70% (Scheme 1, step **v**). **6** was identified by its spectroscopic data and an X-ray diffraction study. The X-ray data were not good enough for a complete solution of the structure. However, the stereochemistry of the framework of this molecule could be clearly identified (Scheme 1). In an earlier publication we reported the reaction of $Re_2(\mu\text{-}H)(\mu\text{-}SH)(CO)_8$ with $Os_3(CO)_{11}(NCMe)$, which leads to $(CO)_8(\mu\text{-}H)Re_2(\mu_4\text{-}S)Os_3(\mu\text{-}H)(CO)_{10}$ (**8**) via the intermediate $(CO)_8(\mu\text{-}H)Re_2(\mu_3\text{-}S)Os_3(\mu\text{-}H)(CO)_{11}$ (**7**).[12] **6** is obviously closely related to the latter molecule, but in **7** the μ_3-S atom is axially (perpendicular to the Os_3 plane) bound to the Os_3 ring, whereas in **6** the μ_3-S ligand is equatorially oriented. This difference in the bonding scheme seems to be the reason for the reactivity of **6** being different from that of **7**. Upon heating under reflux the μ_3-S ligand in **7** substitutes a CO ligand on one of the other osmium atoms, giving the spirocyclic complex **8**.[12] When **6** is treated under the same conditions, only slow decomposition is observed.

The formation of **6** from **5** and $Os_3(CO)_{10}(NCMe)_2$ is a little bit surprising, as the Os_3 ring in **6** is coordinated by 11 CO ligands, whereas the ring in $Os_3(CO)_{10}(NCMe)_2$ coordinates only 10 CO ligands. However, the spectroscopic data of **6** obtained from the reaction with $Os_3(CO)_{10}(NCMe)_2$ and $Os_3(CO)_{11}(NCMe)$, respectively, are identical. Therefore, we assume that the additional CO ligand in the former reaction stems from CO released in the course of accompanying decomposition or side reactions. This assessment is supported by the ^{13}C NMR data of **6**, which show no resonances of free or coordinated acetonitrile. In addition, elemental analy-

sis proves that there is no nitrogen in **6**. Hence, all nitrile ligands have been substituted by sulfur or CO.

The IR spectrum of **6** exhibits 11 ν_{CO} absorption bands, in compliance with the low symmetry of the molecule. The ^{1}H NMR resonance of the μ-H ligand is located at δ −15.21. In the similar complex $(CO)_8(\mu\text{-H})Re_2(\mu_3\text{-S})Os_3(\mu\text{-H})(CO)_{11}$ the corresponding resonance is found at δ −16.38.[12]

Experimental Section

All reactions were performed in solvents free of oxygen, which were dried according to literature methods, distilled, and stored under an argon atmosphere. TLC was carried out on glass plates (20 × 20 cm^2) coated with a mixture of gypsum and silica gel (Merck 60 PF_{254}, 1 mm thick). The reaction products were characterized by ν(CO) FTIR spectroscopy (Nicolet P510, CaF_2 optics) and ^{1}H, ^{13}C, and ^{31}P NMR spectroscopy (Bruker AMX 300).

MeI and CF_3COOH were purchased from Fluka and used as received. $NEt_4[Re_2(\mu\text{-}PCy_2)(CO)_8]$,[18] $Fe_2(\mu\text{-}E_2)(CO)_6$,[23] and $Os_3(CO)_{10+n}(NCMe)_{2-n}$ (n = 0, 1)[24] were prepared according to literature methods.

In Situ Preparation of $NEt_4[(CO)_8(\mu\text{-}PCy_2)Re_2(\mu_4\text{-E})Fe_2(\mu\text{-E})(CO)_6]$ (E = S (2a), Se (2b), Te (2c)). A 140 mg portion (0.151 mmol) of $NEt_4[Re_2(\mu\text{-}PCy_2)(CO)_8]$ was dissolved in 20 mL of THF at room temperature. This solution was added dropwise at −78 °C to a solution of 0.145 mmol of $Fe_2(\mu\text{-}E_2)(CO)_6$ (E = S (50 mg), Se (64 mg), Te (78 mg)) in 10 mL of THF. During this period of time the reaction mixture changes from red to dark green. After the mixture was stirred for another 15 min, accompanying IR and ^{31}P NMR spectra proved the quantitative formation of $NEt_4[(CO)_8(\mu\text{-}PCy_2)Re_2(\mu_4\text{-S})Fe_2(\mu\text{-S})(CO)_6]$ (**2a**). The obtained solutions of **2a**−**c** were used for the consecutively performed reactions. Analytical and spectroscopic data are as follows for **2a** (in situ): IR (THF) $\nu_{C\equiv O}$ 2085 (w), 2067 (s), 2031 (vs), 2006 (vs), 1990 (m), 1945 (m), 1925 (s) cm^{-1}; ^{31}P NMR (THF/C_6D_6) δ −76.0 (s, μ-P).

Preparation of $(CO)_8(\mu\text{-}PCy_2)Re_2(\mu_4\text{-E})Fe_2(\mu\text{-EMe})(CO)_6$ (E = S (3a), Se (3b), Te (3c)). To the above-described solutions of in situ prepared **2a**−**c** was added 18 μL (0.29 mmol) of MeI at −78 °C. The cooling bath was removed and the reaction mixture stirred for 1 h. The resulting orange solution contains a colorless precipitate of NEt_4I. Next the solution was filtered and the solvent removed under reduced pressure. The residue was purified by TLC using dichloromethane/hexane (1/5) as eluent. The obtained orange band afforded 126 mg (75%) of **3a**, 152 mg (84%) of **3b**, and 158 mg (81%) of **3c**, respectively. Analytical and spectroscopic data are as follows for **3a**: IR (CH_2Cl_2) $\nu_{C\equiv O}$ 2098 (w), 2081 (s), 2063 (m), 2036 (vs), 1996 (vs), 1948 (s) cm^{-1}; ^{1}H NMR ($CDCl_3$) δ 1.2−2.1 (m, 22H, Cy), 2.18 (s, 3H, Me); ^{13}C NMR ($CDCl_3$) δ 19.5 (s, Me), 25.7 (s, C^4(Cy)), 27.7 (d, $^2J_{CP}$ = 10 Hz, C^2 or C^6 (Cy)), 27.8 (d, $^2J_{CP}$ = 10 Hz, C^2 or C^6 (Cy)), 35.1 (d, $^3J_{CP}$ = 3 Hz, C^3 or C^5 (Cy)), 35.3 (d, $^3J_{CP}$ = 3 Hz, C^3 or C^5 (Cy)), 42.0 (d, $^1J_{PC}$ = 14 Hz, ^{1}C(Cy)), 186.6 (d, $^2J_{CP}$ = 6.5 Hz, CO (Re)), 187.3 (d, $^2J_{CP}$ = 6.6 Hz, CO (Re)), 189.3 (d, $^2J_{CP}$ = 30.3 Hz, CO (Re)), 189.8 (d, $^2J_{CP}$ = 31.5 Hz, CO (Re)), 192.2 (d, $^2J_{CP}$ = 6.2 Hz, CO (Re)), 193.1 (d, $^2J_{CP}$ = 6.4 Hz, CO (Re)), 208.1 (s, CO (Fe)), 208.9 (s, CO (Fe)); ^{31}P NMR ($CDCl_3$) δ −78.1 (s, μ-P). Anal. Calcd for $C_{27}H_{25}Fe_2O_{14}PRe_2S_2$: C, 28.13; H, 2.19. Found: C, 28.25; H, 2.02. Analytical and spectroscopic data are as follows for **3b**: IR (CH_2Cl_2) $\nu_{C\equiv O}$ 2098 (vw), 2081 (s), 2058 (m), 2033 (vs), 1996 (s), 1950 (s) cm^{-1}; ^{1}H NMR ($CDCl_3$) δ 1.27−2.09 (m, 22H, Cy), 2.16 (s, 3H, Me); ^{13}C NMR ($CDCl_3$) δ 8.7 (s, Me), 25.6 (s, C^4 (Cy)), 27.7 (d, $^2J_{CP}$ = 10 Hz, C^2 or C^6 (Cy)), 27.8 (d, $^2J_{CP}$ = 10 Hz, C^2 or C^6 (Cy)), 35.1 (s, C^3 or C^5 (Cy)), 35.2 (s, C^3 or C^5 (Cy)), 41.9 (d, $^1J_{PC}$ = 12.2 Hz, C^1 (Cy)), 185.7 (d, $^2J_{CP}$ = 7.2 Hz, CO (Re)), 186.4 (d, $^2J_{CP}$ = 7.2 Hz, CO (Re)), 188.4 (d, $^2J_{CP}$ = 33.6 Hz, CO (Re)), 189.4 (d, $^2J_{CP}$ = 33.4 Hz, CO (Re)), 192.3 (d, $^2J_{CP}$ = 6 Hz, CO (Re)), 193.1 (d, $^2J_{CP}$ = 6.4 Hz, CO (Re)), 209.1 (s, CO (Fe)), 209.5 (s, CO (Fe)); ^{31}P NMR ($CDCl_3$) δ −89.1 (t, $^2J_{PSe}$ = 46 Hz, μ-P). Anal. Calcd for $C_{27}H_{25}Fe_2O_{14}PRe_2Se_2$: C, 26.02; H, 2.02. Found: C, 25.90; H, 1.94. Analytical and spectroscopic data are as follows for **3c**: IR (CH_2Cl_2) $\nu_{C\equiv O}$ 2096 (vw), 2077 (s), 2056 (m), 2031 (vs), 1996 (s), 1955 (s) cm^{-1}; ^{1}H NMR ($CDCl_3$) δ 1.29−2.09 (m, 22H, Cy), 2.20 (s, 3H, Me); ^{13}C NMR ($CDCl_3$): −13.8 (s, Me), 25.6 (s, C^4 (Cy)), 27.6 (d, $^2J_{CP}$ = 10 Hz, C^2 or C^6 (Cy)), 27.7 (d, $^2J_{CP}$ = 10 Hz, C^2 or C^6 (Cy)), 35.0 (d, $^3J_{CP}$ = 2.4 Hz, C^3 or C^5 (Cy)), 35.1 (d, $^3J_{CP}$ = 2.4 Hz, C^3 or C^5 (Cy)), 41.7 (d, $^1J_{PC}$ = 10 Hz, C^1 (Cy)), 184.9 (d, $^2J_{CP}$ = 6.3 Hz, CO (Re)), 185.2 (d, $^2J_{CP}$ = 6.4 Hz, CO (Re)), 186.4 (d, $^2J_{CP}$ = 30.7 Hz, CO (Re)), 187.2 (d, $^2J_{CP}$ = 31.2 Hz, CO (Re)), 192.2 (d, $^2J_{CP}$ = 6.2 Hz, CO (Re)), 192.4 (d, $^2J_{CP}$ = 6.3 Hz, CO (Re)), 209.5 (s, CO (Fe)), 210.8 (s, CO (Fe)); ^{31}P NMR ($CDCl_3$) δ −115.3 (s, μ-P). Anal. Calcd for $C_{27}H_{25}Fe_2O_{14}PRe_2Te_2$: C, 24.13; H, 1.88. Found: C, 24.04; H, 1.72.

Preparation of $[(CO)_8(\mu\text{-}PCy_2)Re_2(\mu_4\text{-E})Fe_2(CO)_6]_2(\mu_4\text{-E}_2)$ (E = S (4a), Se (4b), Te (4c)). The above-described solutions of **2a**−**c** were concentrated to 2 mL. Crystallization of **4a**−**c** was achieved by slow diffusion of pentane into these THF solutions in the presence of oxygen (air). The obtained orange crystals of **4a** (153 mg, 93%) are insoluble in all common organic solvents, but they were suitable for X-ray diffraction. The deep red crystals of **4b** (156 mg, 87%) and **4c** (151 mg, 78%), respectively, can be redissolved in THF or $CHCl_3$. Analytical and spectroscopic data are as follows for **4a**: IR (KBr pellet) $\nu_{C\equiv O}$ 2096 (vw), 2083 (m), 2062 (m), 2044 (s), 2006 (s), 1986 (s), 1975 (m), 1946 (vs), 1939 (sh) cm^{-1}. Anal. Calcd for $C_{52}H_{44}Fe_4O_{28}P_2Re_4S_4$: C, 27.45; H, 1.95. Found: C, 27.62; H, 1.85. Analytical and spectroscopic data are as follows for **4b**: IR (CH_2Cl_2) $\nu_{C\equiv O}$ 2096 (vw), 2083 (s), 2060 (m), 2044 (vs), 2009 (sh), 1998 (s), 1952 (s) cm^{-1}; ^{1}H NMR ($CDCl_3$) δ 1.20−2.01 (m, Cy); ^{31}P NMR ($CDCl_3$) δ −83.8 (s, μ-P). Anal. Calcd for $C_{52}H_{44}Fe_4O_{28}P_2Re_4Se_4$: C, 25.38; H, 1.80. Found: C, 25.31; H, 1.72. Analytical and spectroscopic data are as follows for **4c**: IR (CH_2Cl_2) $\nu_{C\equiv O}$ 2096 (vw), 2089 (vw), 2075 (s), 2050 (m), 2031 (vs), 1996 (vs), 1952 (s) cm^{-1}; ^{1}H NMR ($CDCl_3$) δ 1.18−2.09 (m, Cy); ^{31}P NMR ($CDCl_3$) δ −111.5 (s, μ-P). Anal. Calcd for $C_{52}H_{44}Fe_4O_{28}P_2Re_4Te_4$: C, 24.42; H, 1.73. Found: C, 24.35; H, 1.67.

Preparation of $(CO)_8(\mu\text{-}PCy_2)Re_2(\mu_4\text{-S})Fe_2(\mu\text{-SH})(CO)_6$ (5) and $(CO)_8(\mu\text{-}PCy_2)Re_2(\mu_4\text{-S})Fe_2(CO)_6(\mu_3\text{-S})Os_3(\mu\text{-H})(CO)_{11}$ (6). To the above-described solution of **2a** in THF was added 22 μL (0.29 mmol) of CF_3COOH at −78 °C. Then the cooling bath was removed and the solution was stirred until room temperature was reached. The resulting mixture was taken to dryness, giving an orange-red residue. This residue was taken up in dichloromethane and the solution rapidly filtered through silica. The obtained red solution contains pure $(CO)_8(\mu\text{-}PCy_2)Re_2(\mu_4\text{-S})Fe_2(\mu\text{-SH})(CO)_6$ (**5**). This solution was used for the preparation of **6**. A pure, solvent-free sample of **5** was obtained upon removal of the solvent from the aforementioned solution, giving 108 mg (95%) of **5**. It must be noted that the presence of oxygen during isolation of **5** yields a product that is contaminated by the disulfide $[(CO)_8(\mu\text{-}PCy_2)Re_2(\mu_4\text{-S})Fe_2(CO)_6]_2(\mu_4\text{-S}_2)$ (**4a**). The latter is also obtained when the above-mentioned dichloromethane solution of **5** is concentrated under reduced pressure followed by diffusion of pentane into this solution in the presence of aerial oxygen. The crystals of **4a** obtained from this reaction were suitable for X-ray diffraction. To the above-described solution of **5** in dichloromethane was added 133 mg (0.145 mmol) of $Os_3(CO)_{11}(NCMe)$ at room temperature. The mixture was stirred for 3 h. Removal of the solvent under reduced pressure gave a reddish brown residue that was subjected to TLC using dichloromethane/hexane (1/2) as eluent. The only observed band afforded 139 mg (70%) of reddish brown $(CO)_8(\mu\text{-}PCy_2)Re_2(\mu_4\text{-S})Fe_2(CO)_6(\mu_3\text{-S})Os_3(\mu\text{-H})(CO)_{11}$ (**6**). Analytical and spectroscopic data are as follows for **6**: IR (CH_2Cl_2) $\nu_{C\equiv O}$ 2112 (w), 2092 (w), 2079 (s), 2060 (m), 2048 (m), 2033 (vs), 2023 (sh),

2013 (sh), 1992 (s), 1975 (m), 1940 (m) cm^{-1}; ^1H NMR ($CDCl_3$) δ −15.21 (s, 1H, μ-H), 1.3−2.2 (m, 22H, Cy); ^{13}C NMR ($CDCl_3$) δ 25.8 (s, C^4(Cy)), 27.5−28.0 (m, C^2 and C^6 (Cy)), 35.1−35.5 (m, C^3 and C^5 (Cy)), 41.4 (d, $^1J_{CP}$ = 13 Hz, C^1(Cy)), 42.2 (d, $^1J_{CP}$ = 13 Hz, C^1(Cy)), 168.7−173.6 (m, CO (Os, Re)), 181.8−193.0 (m, CO (Os, Re)), 210.9 (s, CO (Fe)), 211.0 (s, CO (Fe)); ^{31}P NMR ($CDCl_3$) δ −72.2 (s, μ-P). Anal. Calcd for $C_{36}H_{23}Fe_2O_{24}Os_3PRe_2S_2$: C, 21.74; H, 1.17. Found: C, 21.90; H, 1.24.

Crystal Structure Determinations. Crystals suitable for X-ray analysis for compounds **3a**−**c** and **4a**−**c** were obtained from chloroform/pentane, THF/pentane or dichloromethane/pentane solutions. Pertinent crystallographic data are summarized in Tables 1 and 2. Data sets for **3c** and **4b**,**c** were collected on a Bruker SMART APEX diffractometer and all other data sets on a Bruker P4 diffractometer with Mo Kα radiation each. Data reduction was carried out with standard methods from the software packages Bruker SAINT[27] and Bruker XSCANS,[28] respectively. P4 data were corrected for absorption via ψ scans, and SMART data were treated with SADABS.[27] The structures were solved by direct and conventional Fourier methods. Full-matrix least-squares refinement was based on F^2. All but the hydrogen atoms were refined anisotropically; geometrically placed hydrogen atoms were refined with a riding model and $U(H) = 1.2[U(C_{iso})]$. Programs used for calculations: SHELXTL.[27]

(27) SMART (version 5.62), SAINT (version 6.02), SHELXTL (version 6.10), and SADABS (version 2.03); Bruker AXS Inc., Madison, WI, 2000.

(28) XSCANS (version 2.31); Bruker AXS Inc., Madison, WI, 1999.

Supporting Information Available: Tables of refined atomic coordinates, bond lengths and angles, anisotropic thermal parameters, and calculated hydrogen atomic coordinates for **3a**−**c** and **4a**−**c**; these data are also available as CIF files. This material is available free of charge via the Internet at http://pubs.acs.org.

OM030200U